Front. Optoelectron. China 2010, 3(2): 163–168
DOI 10.1007/s12200-010-0008-x

RESEARCH ARTICLE

Evaluation of Er,Cr:YSGG laser for hard tissue ablation: an *in vitro* study

Xianzeng ZHANG (✉)[1], Shusen XIE[1], Zhenlin ZHAN[1], Haibin ZHAO[1], Jian GUO[1], Qing YE[2,3]

1 Institute of Laser and Optoelectronics Technology, Fujian Provincial Key Laboratory for Photonics Technology, Key Laboratory of OptoElectronic Science and Technology for Medicine of Ministry of Education, Fujian Normal University, Fuzhou 350007, China
2 Department of Otolaryngology, Fujian Provincial Hospital, Fuzhou 350001, China
3 Fujian Provincial Clinical College, Fujian Medical University, Fuzhou 350001, China

Abstract The use of erbium,chromium:yttrium-scandium-gallium-garnet (Er,Cr:YSGG) laser with a wavelength of 2.78 μm for hard bone tissue ablation was evaluated. The surface morphology and microstructure changes of bone tissue treated with Er,Cr:YSGG were analyzed as compared to those treated with diamond drill. The influence of fluence on ablation rate and ablation efficiency as well as microstructure was also examined. The results show that Er,Cr:YSGG laser can perform bone perforation that is more fine and presented a lot of unique advantages compared to traditional methods. An approximately linear relationship was observed between the ablation rate/ablation efficiency and radiant exposure. Increasing the radiant exposure irradiated on bone tissue will produce stronger thermal injury around the crater and result in microstructure changing.

Keywords tissue ablation, erbium,chromium:yttrium-scandium-gallium-garnet (Er,Cr:YSGG) laser, bone, evaluation technology

1 Introduction

Hard tissue cutting or drilling with laser systems has extensive applications in bone surgery and dentistry and has been paid more and more attention to in recent years [1–11]. Compared to traditional methods including saw and drill in today's medical practice, laser hard tissue processing in a no-contact operating model can provide a lot of unique advantages such as no vibration and mechanical defects, no bone dust, easy control or operation, more precise and comfortable, and clear visual field. Therefore, laser has been considered as one of the most promising tools in the future to compensate/substitute the traditional instruments for the cutting or processing of hard biological tissue. Especially in dentistry, it has been believed to have the potential to be a major innovation.

The ideal laser for bone cutting would be capable of high ablation rate with high pulse repetition rate to remove large tissue volumes in a short time, and at the same time would be capable of minimizing peripheral thermal injury around the cuts to prevent delayed wound healing. The main infrared (IR) energy absorbers for compact bone are carbonated hydroxyapatite (accounted for 65% by mass), water (10%) and collagen (25%) [4,12]. Previous studies have shown that erbium:yttrium-scandium-gallium-garnet (Er:YAG) and CO_2 lasers may be the most suitable candidates for practical application due to the strong absorption peaks of water and carbonated hydroxyapatite overlap with the Er:YAG (2.94 μm) and CO_2 (9.6 and 10.6 μm) laser wavelengths, respectively. Although a wavelength operating at 6.1 μm emitted from free-electron laser may produce the largest crater area with the least amount of collateral thermal injury compared to 2.9 and 6.45 μm due to highly optical absorption by both protein ($\mu_a = 2700\ cm^{-1}$) and water ($\mu_a = 8480\ cm^{-1}$) [4], its clinical utility has been limited because there is no practicable laser source available at this wavelength.

In recent years, another available laser system suggested for hard tissue ablation is the erbium,chromium:yttrium-scandium-gallium-garnet (Er,Cr:YSGG). This laser is a kind of erbium laser (2.69–2.94 μm) similar to Er:YAG (2.94 μm), erbium:lithium yttrium fluoride (Er:YLF) (2.81 μm), erbium:yttrium aluminum perovskite (Er:YAP) (2.73 μm), and chromium, thulium, erbium, yttrium, aluminum garnet (CTE:YAG) (2.69 μm), and emits light in the mid-infrared region at 2.78 μm. Although the room temperature absorption coefficient at 2.78 μm is

Received October 24, 2009; accepted December 23, 2009

E-mail: xzzhang@fjnu.edu.cn

$\mu_a = 5300\ cm^{-1}$, which is less than half the absorption coefficient at 2.94 μm ($\mu_a = 12500\ cm^{-1}$), the additional absorption of Er,Cr:YSGG laser by the OH^- group in the carbonated hydroxyapatite mineral of the bone make it an alternative laser system for safe and efficient hard tissue ablation [13,14]. The mechanism of hard tissue removal by this laser is called a "thermo-mechanical process" in which the emission laser light is absorbed by the OH^- groups of free water and hydroxyapatite of hard tissue. The water is then heated and evaporated, resulting in a high pressure of steam that causes a microexplosion of hard tissue below the melting point of hard tissue (approximately 1200°C).

Up to now, studies or applications of Er,Cr:YSGG laser were largely focused on dental hard tissue; its ablation characteristics on bone hard tissue has not yet appeared and this is the goal in the present work. In order to evaluate the ability of Er,Cr:YSGG laser to perform bone tissue cutting or perforating, the surface morphological and microstructural changes of bone tissue after Er,Cr:YSGG laser irradiation with various radiant exposure were compared to those after conventional bur drilling, which has been performed as an acceptable method for bone surgeries in today's medical practice. The influence of radiant exposure on ablation rate and ablation efficiency, and the correlation between them were studied. Laser-induced thermal injury and microstructure on bone tissue with various radiant exposures were also examined.

2 Materials and methods

Fresh bovine tibia obtained no later than 6 h post-mortem from a local slaughterhouse was used for *in vitro* laser-tissue ablation experiments. The bone specimens were rinsed in tap water to remove hemocytes after the connective tissue and periosteum were peeled away with a razor blade. Then the tibia was cut into rectangular blocks (~2 cm×4 cm with original compact thickness) with a diamond saw. In order to obtain a flat surface, the sample surface was polished using sandpaper with a grain size of 30 μm followed by ultrasonic cleaning to remove the smear layer, and then the prepared samples were stored in a saline solution at 4°C prior to experimentation to prevent dehydration.

The light source used for hard tissue ablation in the study is Er,Cr:YSGG laser (Waterlase, Biolase Technology Inc., San Clemente, CA, USA) operating at a wavelength of 2.78 μm with a pulse duration of 140 μs, a fixed pulse repetition rate of 20 Hz and a power output range of 0 to 6 W. Laser light was delivered through a fiber optic system to a sapphire tip terminal with a diameter of 400 μm and a divergence of 8°, and then irradiated perpendicularly on bone sample. A built-in water spray system was also used to produce a flow rate of 0.5 mL/s as laser ablating. The bone sample was placed on a sample holder which was controlled by an *XYZ*-stage permitting to maintain approximately 1 mm distance between tip and tissue surface for all the experiments. A schematic illustration of the experimental setup is shown in Fig. 1. The actual beam diameter incident on tissue surface was about 540 μm. Samples were lased for 10 s in non-contact mode with power setting from 0.5 W (pulse energy 22.5 mJ) to 2.5 W (pulse energy 112.5 mJ) in a step of 0.5 W, meaning that a total of 200 pulses were impacted on one crater. A total of 25 specimens were irradiated in the experiment. The exact fluence was measured by an energy meter (NOVA Ⅱ, Orphir, Israel) along with a pyroelectric joulemeter (PE50-BB-SH-V2, Orphir). The output pulse energy was measured before and after every bone ablation test. The fiber tip was replaced if the measured energy was reduced by more than 15% of the initial output energy to avoid experimental artifacts due to fiber damage. Furthermore, a bone cutting experiment performed by an electrically driven diamond drill (MD20, Nouvag, Switzerland) with a diameter of 0.5 mm was conducted as control group. The drill was set with gentle pressure against the bony wall turning at 1000 revolutions per minute. The operation time for each crater was set at 10 s.

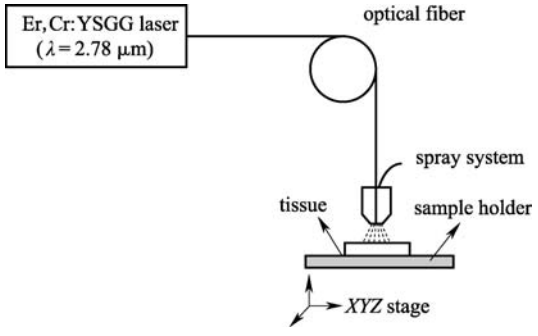

Fig. 1 Experimental setup for bone ablation study with Er,Cr:YSGG laser (note the 1 mm distance between fiber tip and tissue surface)

After irradiation, surface profile and morphological changes of ablative bone were examined using a stereomicroscope (MZ16FA, LEICA, Germany). Cross-section imaging of the ablated crater was taken by an optical coherence tomography (OCT) system ($\lambda_0 = 850$ nm, $\Delta\lambda = 50$ nm, and $P = 7$ mW) with lateral and axial resolutions of ~10 μm, and the ablation depth was measured with a self-compiled program. Then the treated specimens were further detected with a scanning electron microscope (XL30 ESEM, FEI, Netherland) operating at 30 kV after serial processing of dehydration and gold coating. The scanning electron microscope (SEM) images were taken from different parts of the incisions under various magnifications. Morphological alterations and microstructural changes of treated specimens were valued.

3 Results and discussion

Stereomicroscope top-view images of crater created on bone sample by diamond drill (Fig. 2(a)) and Er,Cr:YSGG laser (Fig. 2(b)) with a radiant exposure of 39.3 J/cm^2 are shown in Fig. 2. Diamond drill as a standard tool in today's medical practices can perform bone perforating or drilling efficiency. As shown in Fig. 2(a), the crater made by diamond drill presents a clear and regular sharpness with debris distributing randomly around the edge. Bone perforating was always accompanied with vibration, mechanical friction and debris ejecting. The quality of the crater was mainly depending on the skill and experience of the operator. As for the laser system, the crater created by Er,Cr:YSGG laser as shown in Fig. 2(b) presents a profile of sharp edge, regular shape and clear surface. No obvious debris was found around the crater. No vibration and mechanical defects occurred during laser-tissue interaction. Moreover, this kind of no-contact technique produced a lot of benefits compared to traditional methods such as no bone dust, easy control or operation, more precise and comfortable, and clear visual field.

The depth of laser-induced craters on bone samples as a function of incident radiant exposure is illustrated in Fig. 3. The error bars present the standard deviations of the data. The real line is a linear fitting line. The total pulse number impacted in one crater was set at 200. It is shown that there is an approximately linear relationship ($R^2 = 0.96$) between the ablation depth and incident radiant exposures. As shown in Fig. 3, the crater depth increased from about 42 μm at 9.8 J/cm^2 up to 690 μm at 49 J/cm^2.

Ablation rate is one of the main quantities to feature laser-induced tissue ablation. In the study, ablation rate (ablation depth per pulse) varied with radiant exposure is produced in Fig. 4(a). It shows that ablation rate increased monotonously with the incident radiant exposure. Higher ablation rate means that a larger volume of tissue can be ablated at each pulse and less time will be consumed for hard tissue perforating operation. Although a lower ablation rate will produce a more precise outcome, the perforating operation will consume too much time. Therefore, there is a balance between higher quality outcome and less operation time. One can improve ablation rate simply by increasing radiant exposure and/or pulse repetition number, and vice versa.

Another key quantity to characterize tissue ablation with laser is ablation efficiency, which can be defined in terms of the amount of tissue within the given time, the volume removed per joule of energy incident on the tissue (mm^3/J), and the volume ablated per second (mm^3/s). In the study reported, the ablation efficiency was defined as crater depth ablated per unit energy. Figure 4(b) indicates the correlation of laser-induced crater depth per unit energy as a function of incident radiant exposure. It shows that ablation depth per unit energy increases monotonously with the increasing of radiant exposure. This means that although the same total energy was applied to the target tissue, higher ablation efficiency can be obtained with higher radiant exposure.

Surface morphology and microstructure changes of bone sample after treatment with different methods are evaluated with scanning electron micrograph and presented in Fig. 5. Figures 5(a) and 5(b) indicate the edge and base of the crater created by a diamond drill, respectively; Figures 5(c) and 5(d) indicate the edge of the crater ablated by Er,Cr:YSGG laser at 29.5 and 49.2 J/cm^2, respectively. As shown in Fig. 5(a), the craters perforated by diamond drill present a helical profile with sharp-cut edge and rough surface. Circular shape mechanical scratch can be observed obviously on the crater wall which was induced by uneven stress during the manipulation of the diamond drill, and this kind of mechanical defect was ineluctable in practice. A loose smear layer covered the entire crater surface with bone debris attached on it. Large bone fragments were accumulated on the bottom of the

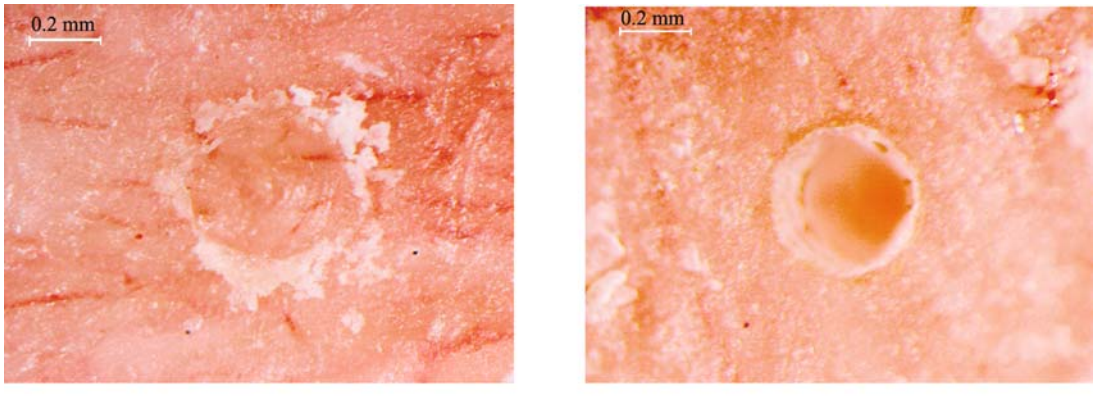

Fig. 2 Stereomicroscope top-view images of crater on bone sample created by different methods. (a) Diamond drill; (b) Er,Cr:YSGG laser at 39.3 J/cm^2 (length of bar is 200 μm)

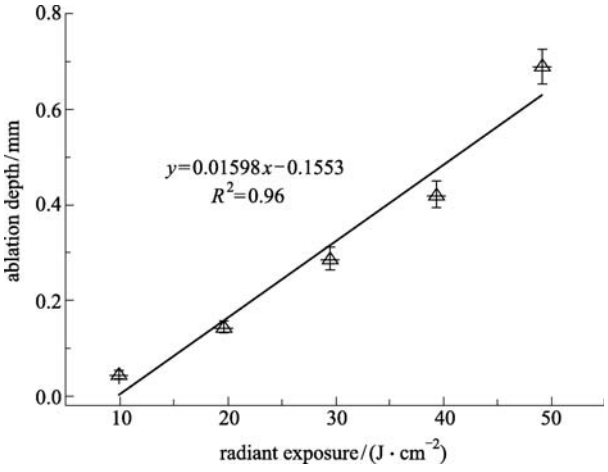

Fig. 3 Ablation depth of crater created on bovine shank bone by Er,Cr:YSGG laser as a function of incident radiant exposure (error bars are standard deviations of the data)

crater, and crack was found clearly on the base (Fig. 5 (b)). In contrast, the crater appearance after the laser irradiation indicated a corrugated or Volcano-like profile (Figs. 5 (c) and 5(d)) at all energy settings. There was a transition layer of thermal injury with a thickness of about 10 μm between the irradiated site and untreated tissue. As shown in Fig. 5(c), white particles with an appearance of condensed droplets distributed randomly around the crater edge can be observed clearly. The size of these particles ranged from about several μm to 10 μm which correspond to the dimensions of apatite crystallites, the main components in bone tissue [15]. A melting layer looking like volcanic rock distributed on the inside wall of the laser-induced crater which might have been induced by the recrystallization of the original apatites after laser irradiation. With the increasing of applied radiant exposure, the thickness of thermal injury layer around the crater edge grew up gradually. As shown in Fig. 5(d), the altered layer grows up to about 30 μm at a radiant exposure of 49.2 J/cm^2, three times of the one at 29.5 J/cm^2. White particles disappear and fusion of the original apatites was observed resulting in huge amorphous structures with an appearance of honeycomb which covered the entire crater surface.

4 Conclusion

The ability of Er,Cr:YSGG laser for hard bone tissue ablation and the surface morphology and microstructure changes of crater induced by multi-pulses, as well as the applied radiant exposure effects were evaluated in the present work. Er,Cr:YSGG laser can produce a finer crater with an appearance of sharp edge, regular and clear surface compared to traditional methods. Furthermore, the no-contact technology can provide a lot of unique advantages such as no vibration and mechanical defects, no bone dust, easy control or operation, more precise and comfortable, and clear visual field. By increasing incident radiant exposure, higher ablation rate and ablation efficiency will be obtained with stronger thermal injury. Energy parameter also has an important influence on the microstructure changes of laser induced craters. Further work will focus on the enhancement of ablation rate and ablation efficiency, minimizing thermal injury and the influence of the morphology and microstructure changes on bone healing.

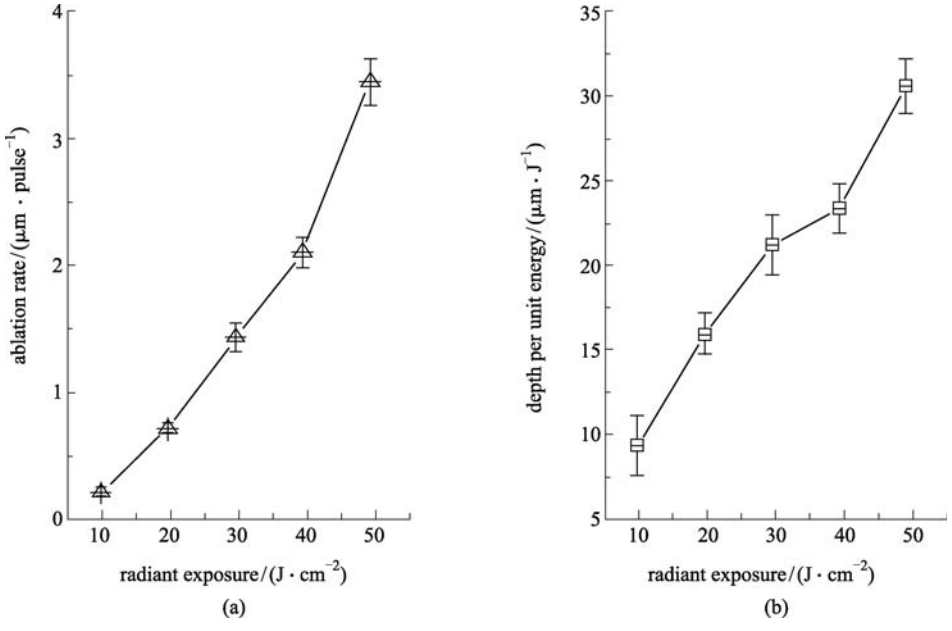

Fig. 4 Ablation rate and ablation depth per unit energy as a function of incident radiant exposure (error bars are standard deviations of the data). (a) Ablation rate; (b) depth per unit energy

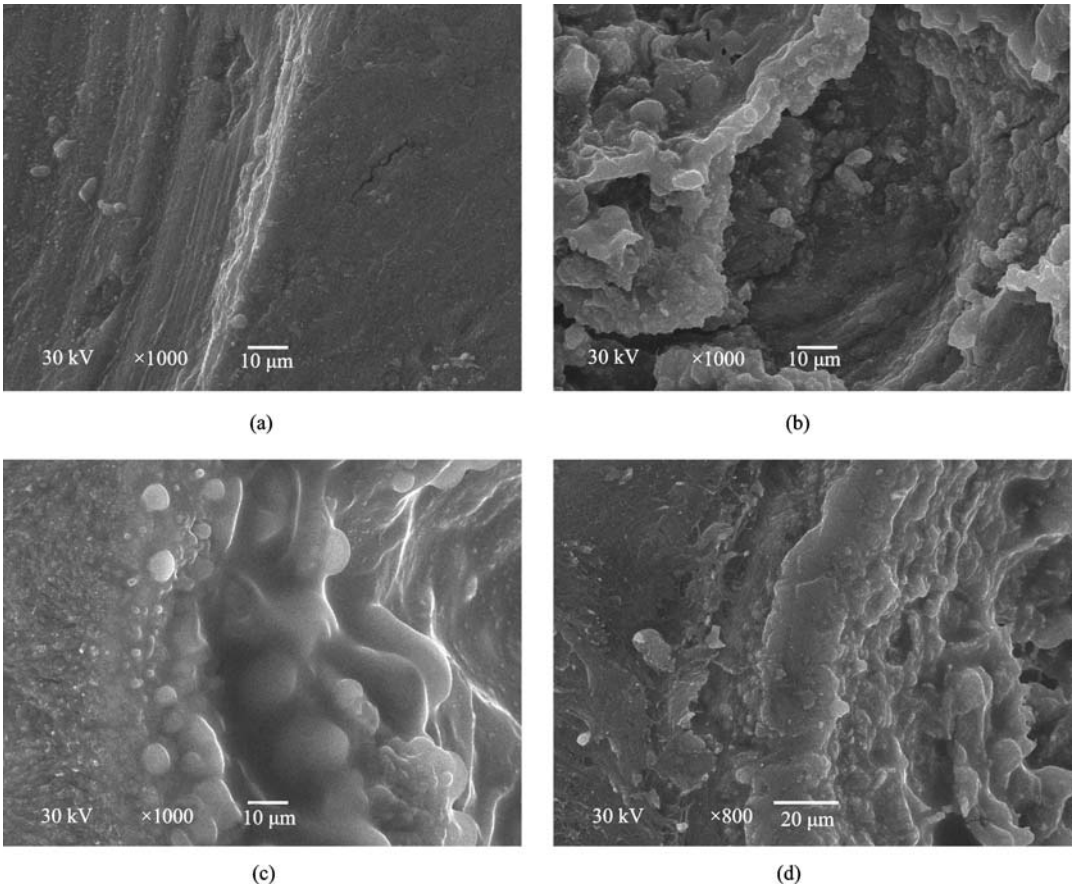

Fig. 5 SEM photomicrographs of craters created on bone with different methods. (a) Edge of crater created by diamond drill; (b) base of crater created by diamond drill; (c) edge of crater ablated by Er,Cr:YSGG laser at 29.5 J/cm^2; (d) edge of crater ablated by Er,Cr:YSGG laser at 49.2 J/cm^2

Acknowledgements This project was supported partly by the National Natural Science Foundation of China (Grant Nos. 60578057 and 60878062), Natural Science Foundation of Fujian Province (No. 2008J0317), and Project WKJ2008-2-035 supported by Science Research Foundation of Ministry of Health, and United Fujian Provincial Health and Education Project for Tackling the Key Research, P. R. China, respectively.

References

1. Meister J, Franzen R, Gavenis K, Zaum M, Stanzel S, Gutknecht N, Schmidt-Rohlfing B. Ablation of articular cartilage with an erbium: YAG laser: an *ex vivo* study using porcine models under real conditions-ablation measurement and histological examination. Lasers in Surgery and Medicine, 2009, 41(9): 674–685
2. Shahar R, Weiner S. Insights into whole bone and tooth function using optical metrology. Journal of Materials Science, 2007, 42(21): 8919–8933
3. Werner M, Ivanenko M, Harbecke D, Klasing M, Steigerwald H, Hering P. Laser osteotomy with pulsed CO_2 lasers. Advances in Medical Engineering, 2007, 114: 453–457
4. Youn J I, Sweet P, Peavy G M. A comparison of mass removal, thermal injury, and crater morphology of cortical bone ablation using wavelengths 2.79, 2.9, 6.1, and 6.45 microm. Lasers in Surgery and Medicine, 2007, 39(4): 332–340
5. Youn J I, Sweet P, Peavy G M, Venugopalan V. Mid-IR laser ablation of articular and fibro-cartilage: a wavelength dependence study of thermal injury and crater morphology. Lasers in Surgery and Medicine, 2006, 38(3): 218–228
6. Ivanenko M, Sader R, Afilal S, Werner M, Hartstock M, Von Hänisch C, Milz S, Erhardt W, Zeilhofer H F, Hering P. *In vivo* animal trials with a scanning CO_2 laser osteotome. Lasers in Surgery and Medicine, 2005, 37(2): 144–148
7. Ivanenko M, Werner M, Afilal S, Klasing M, Hering P. Ablation of hard bone tissue with pulsed CO_2 lasers. Medical Laser Application, 2005, 20(1): 13–23
8. Frentzen M, Götz W, Ivanenko M, Afilal S, Werner M, Hering P. Osteotomy with 80-μs CO_2 laser pulses: histological results. Lasers in Medical Science, 2003, 18(2): 119–124
9. Ivanov B, Hakimian A M, Peavy G M, Haglund R F Jr. Mid-infrared laser ablation of a hard biocomposite material: mechanistic studies of pulse duration and interface effects. Applied Surface Science, 2003, 208–209: 77–84
10. Ivanenko M M, Fahimi-Weber S, Mitra T, Wierich W, Hering P. Bone tissue ablation with sub-μs pulses of a Q-switch CO_2 laser:

histological examination of thermal side effects. Lasers in Medical Science, 2002, 17(4): 258–264

11. Fried N M, Fried D. Comparison of Er:YAG and 9.6-microm TE CO_2 lasers for ablation of skull tissue. Lasers in Surgery and Medicine, 2001, 28(4): 335–343
12. Forrer M, Frenz M, Romano V, Altermatt H J, Weber H P, Silenok A, Istomyn M, Konov V I. Bone-ablation mechanism using CO_2 lasers of different pulse duration and wavelength. Applied Physics B, 1993, 56(2): 104–112
13. Featherstone J D B, Fried D. Fundamental interactions of lasers with dental hard tissues. Medical Laser Application, 2001, 16(3): 181–194
14. Kang H W, Rizoiu I, Welch A J. Hard tissue ablation with a spray-assisted mid-IR laser. Physics in Medicine and Biology, 2007, 52 (24): 7243–7259
15. Izatt J A, Albagli D, Britton M, Jubas J M, Itzkan I, Feld M S. Wavelength dependence of pulsed laser ablation of calcified tissue. Lasers in Surgery and Medicine, 1991, 11(3): 238–249